Catalysis Today 147S (2009) S149–S155

Contents lists available at ScienceDirect

Catalysis Today

journal homepage: www.elsevier.com/locate/cattod

Experimental and modelling aspects in microstructured reactors applied to environmental catalysis

J.R. Hernández Carucci *, K. Eränen, D.Yu. Murzin, T.O. Salmi

Laboratory of Industrial Chemistry and Reaction Engineering, Process Chemistry Centre, Åbo Akademi University, FI-20500, Turku/Åbo, Finland

ARTICLE INFO

Article history:
Available online 3 August 2009

Keywords:
Microreactor
Modelling
NOx reduction
Ag/Al_2O_3
Biodiesel

ABSTRACT

Shallow microchannels (Ø = 460 μm, length = 9.5 mm, and depth 75 μm) were successfully coated with an Ag/Al_2O_3 catalyst by washcoating. The coated microchannels were characterized and tested for the selective catalytic reduction (SCR) of NOx, using a simulated diesel engine exhaust in the temperature range of 150–550 °C at atmospheric pressure. Hexadecane, which is regarded as a high-quality diesel fuel, was used as reducing agent.

The prediction of flow characteristics inside the microchannels was done by a two-dimensional finite element model and computational fluid dynamics (CFD) simulations. Theoretical calculations of the microchannels were done to describe the concentration profiles in the radial direction. The dynamic model consisting of a system of partial differential equations was discretized using a finite difference formulation with respect to the spatial coordinate. The resulting ordinary differential equations were solved with backward difference method to guarantee stability and convergence. The concentration profiles of the reactants ($C_{16}H_{34}$, NO) and products (CO_2, N_2) of the HC-SCR system were calculated. The outcome indicates that a rigorous model for microchannels coated with a catalyst layer of variable thickness can be obtained to evaluate the reactive flow inside the channels.

1. Introduction

Microstructured reactors open a new perspective to chemical technology and reaction engineering offering high surface-to-volume ratio, very efficient heat and mass transfer along with intrinsic safety [1]. Microreactors can be used both as research instruments in laboratory scale to enhance the development of new catalysts and processes and for the determination of reaction kinetics as well as real production units in large scale. In the future, dangerous and unstable chemicals are not going to be transported on the roads, but manufactured on site, where they are needed. With microreactors, fine chemicals can be produced in a continuous mode, thus enabling stable operation conditions and a high product quality. It is expected that many chemical processes carried out batchwise today will be performed in continuous microreactors in the future.

On the other hand, the growing concern for the environment and the strict legislation regarding mobile source emissions has led to the emergence of the research in environmental catalysis. New and stronger evidence has been found that most of the global warming over the last 50 years is attributable to human activities. These activities have altered the chemical composition of the atmosphere through the build-up of greenhouse gases – primarily carbon dioxide, methane, and nitrous oxide. At the same time, it has become of imperative importance to develop new and effective ways to reduce the emissions of these gases that are affecting our living environment. After the 1997 Kyoto Protocol, the world has finally taken the first major step in reducing gaseous emissions. Bio-derived fuels are regarded as an alternative for the problem, especially for reducing the oil dependence in the transport sector. Since biofuels produce more NOx than petrodiesel in combustion, its use as a fuel requires a precise understanding of NOx reduction. Regarding the higher content of P and K in bio-derived fuels, when producing high-quality biodiesels, the unwanted components are usually removed prior production (for example, P is removed before hydrodeoxygenation when producing NExBTL, yielding a high-quality diesel consisting mainly of linear alkanes) [2].

Three major catalytic techniques are widely proposed and used for removal of NOx emissions from lean-burn and diesel operated vehicles: NOx-storage, Urea-SCR and HC-SCR. Each technique has significant disadvantages such as sulphur sensitiveness and regeneration requirements of NOx-storage materials, infrastructure issues and formation of ammonium nitrate (at low temperatures) for urea-SCR and low temperature activity of HC-SCR catalysts. For a car manufacturer, a technically attractive method is the HC-SCR, which makes use of existing hydrocarbons

* Corresponding author.
E-mail address: johernan@abo.fi (J.R. Hernández Carucci).

0920-5861/$ – see front matter © 2009 Elsevier B.V. All rights reserved.
doi:10.1016/j.cattod.2009.07.034

in the exhaust (passive control) or added fuel (active control) in front of the converter to reduce NOx. However, most of the materials developed for this technique suffer from almost non-existing low-temperature activity, Pt/alumina being an exception. Yet, this catalyst has a very narrow activity window and a tendency to selectively produce N_2O. Ag/Al_2O_3 has been found to be one of the most active catalysts for the NO-to-N_2 conversion up to date [3–5], and challenges remain more on the reduction at low temperatures (<350 °C). However, copper-exchanged zeolites have been found to be active at low temperatures [6,7] and can be used in combination with Ag/Al_2O_3 catalysts [8]. Moreover, additional reductants, e.g., hydrogen in small quantities, have been found to enhance dramatically the NO-to-N_2 conversion at low temperatures [9–11].

The exhaust treatment of conventional fuels has been discussed in detail in several publications as Burch et al. have presented in their review article [12]. In the future, however, the crucial issue resides in how to clean the emissions from biofuels. There, catalytic development alone is not sufficient, but very precise kinetic and mathematical studies are necessary. For this purpose, microreactors provide an excellent alternative.

To our knowledge, no comprehensive study which generalizes the mass balance in a microchannel and its catalytic layer, solving the fully coupled problem of chemical reactions with a laminar flow model including radial diffusion and diffusion in the catalyst layer has been conducted yet. With this work, we make an attempt to close this gap, using as an application case the HC-SCR.

Many similarities between the microreactor used in this work and conventional monoliths exist. Hayes and Kolaczkowski have investigated the heat and mass transfer limitations for the oxidation of hydrocarbons in monolithic reactors [13]. Recently, Hayes et al. [14] have also investigated the effect of different washcoats in square channels for monolith reactors used in automobile exhaust gas. As early as 1992 Tronconi et al. developed a model for SCR catalytic converters [15], further implementing different levels of modelling [16] and even studying different channel shapes [17]. Other efforts for the NOx reduction using ammonia have also been conducted [18]. In principle, some of the models developed for monolith channels, where laminar flow is present are valid for microreactors. Still, some simplifications could be made when operating with microdevices and etched shapes on the channels. Firstly, due to the high surface-to-volume ratio, the reactor works at constant temperatures, eliminating the need of energy balances. Regarding the mass transfer, when comparing traditional monoliths and our microdevice, the main differences are in the edges and the characteristic lengths. The characteristic length on semi-elliptical channels could be assumed as the maximum distance from the centre of the channel (molecules with the highest velocity) to the washcoat, hence, overestimating the mass transfer limitations compared to the real channel when the simulations are performed. This assumption could be done due to the semi-elliptical shape of the channel. For traditional monoliths that are usually of rectangular shapes, the effect of the sharp edges on the mass transfer cannot be neglected.

2. Experimental

2.1. Preparation of the active phase

In order to use microstructures for catalytic screening there is a need to introduce an active catalytic phase. Among the most common coating techniques one can find anodic oxidation, sol-gel method, chemical vapour deposition and washcoating [19]. A 1.5 wt.% Ag/alumina catalyst was obtained by the latter plus metal impregnation. The mass of the catalyst deposited on each plate was 0.7 mg and its surface area was found to be 70 m^2/g [20].

The detailed preparation and characterization of the catalyst used in this study is presented elsewhere [20].

2.2. Experimental set-up

The gas-phase microreactor was designed at Åbo Akademi and the parts were purchased from Institut für Mikrotechnik Mainz GmbH (IMM). The device consists of a two-piece cubic chamber with two inlets and one outlet, each with a tube diameter of 710 μm. The lower part of the chamber has two recesses, each filled with a stack of 10 stainless steel (before the catalytic coating) micro-structured plates, which are connected by a diffusion tunnel, where the gases from the two reactor inlets mix before entering into the catalytic area (Fig. 1, left). The first stack contains a total of 10 mixing plates with 9 semicircular channels of different radii but with a common centre. They are arranged in the stack in such a way that they meet the two inlets in alternation. The second stack, the catalytic zone of the reactor consists of 10 rectangular plates with 9 parallel shallow microchannels each (total of 90 microchannels: Ø = 460 μm, length = 9.5 mm and depth = 75 μm) coated with an Ag/Al_2O_3 catalyst. The washcoat thickness was determined to be between 15 and 20 μm as revealed by SEM micrographs. Fig. 1, right, shows a scheme of the plates' configuration inside the microreactor. Pressures and temperatures up to 50 bar and 600 °C, respectively, can be achieved.

2.3. Kinetic experiments

The kinetic experiments were carried out in a typical catalytic set-up with a microreactor containing the 1.5 wt.% Ag/Al_2O_3-coated microplates. The microreactor chamber was connected to a temperature controller (CAL Controls 9500P) and k-type thermocouples for monitoring the temperature in the catalytic area. Before each kinetic experiment, the microplates were pre-treated

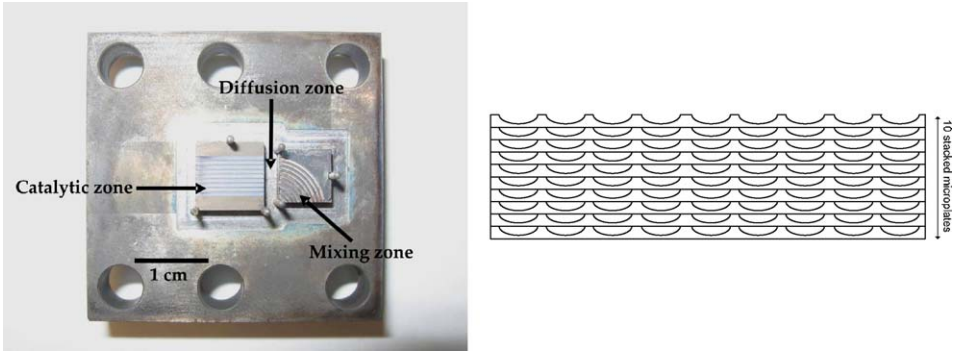

Fig. 1. Microreactor chamber (mixing and catalytic zones, left) and scheme of the reactor configuration (10 stacked microplates, catalytic zone, left).

under 6 vol.% O_2 flow in helium for 30 min. The experiments were carried out under atmospheric pressure and the temperature was varied linearly from 150 to 550 °C, with an interval of 50 °C. The samples were taken 20 min after stabilizing the reaction temperature to guarantee isothermal steady state conditions. No deactivation of the catalyst was observed. For each temperature, the concentrations of the reactants in the gas flow were varied as follows: (a) keeping the concentrations of hexadecane and oxygen at 187.5 and 60,000 ppm respectively, NO was varied (750, 1000, 1500, 2000 ppm); (b) keeping the concentrations of NO and oxygen at 500 and 60,000 ppm, hexadecane was varied (187.5, 375, 468.8 ppm); and (c) keeping the concentration of hexadecane and NO at 187.5 and 500 ppm, respectively, the oxygen variation was done (3, 4.5, 9, 12, and 15 vol.%). The concentration of water was kept constant at 12 vol.% in all the cases. Helium was used for balance. A total of 132 experiments were performed (12 different conditions at each temperature). The total gas-flow rate was always kept at 50 ml/min.

NO was fed from a mixture of 5.01 mol% NO in helium. All the gases were of high purity (AGA) and were pre-heated to 100 °C and introduced into the reactor by means of mass flow controllers (Brooks 5850). The liquid flows, i.e., water and hexadecane, were pumped via a syringe pump (CMA/102 Microdialysis). Due to the small amounts of hexadecane present during the experiments (187.5–468.8 ppm), it was assumed to be vaporised on the gas stream even at temperatures lower than its boiling point (287 °C). The liquids were condensed after the reactor, prior introduction of the gases to the GC.

The concentrations of the resulting species were determined by a Hewlett-Packard Gas Cromatograph (GC) System 6890 series with TC and FI detectors. The NOx, NO and NO_2 concentrations were measured by a PPM Systems Chemiluminescent NOx Analyzer model 200AH. High-purity calibration gases (AGA) were used for calibration of the NOx analyzer and the GC.

3. Results and discussion

3.1. Catalyst characterization

The plates were characterized by scanning electron micrographs with energy dispersive X-ray analysis (SEM-EDXA), laser ablation-inductively coupled plasma-mass spectrometry (LA-ICP-MS) and X-ray photoelectron spectroscopy (XPS). The silver loading with respect to Al_2O_3 was found to be 1.5 wt.% and the metal content was found to be uniform along the channel [20]. SEM micrographs were used for determining the thickness of the catalytic layer, which was found to be ca. 16 μm close to the centre of the channel but varied between 15 and 20 μm (Fig. 2). Detailed characterization information of the catalyst is found elsewhere [19–21].

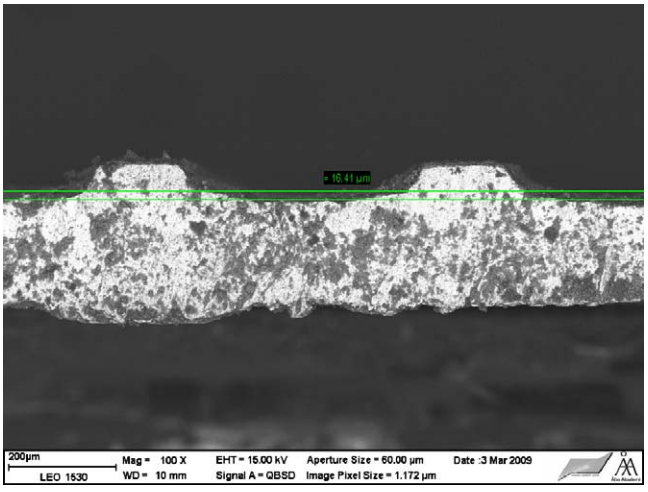

Fig. 2. SEM micrograph of an Ag/alumina-coated microplate (100×).

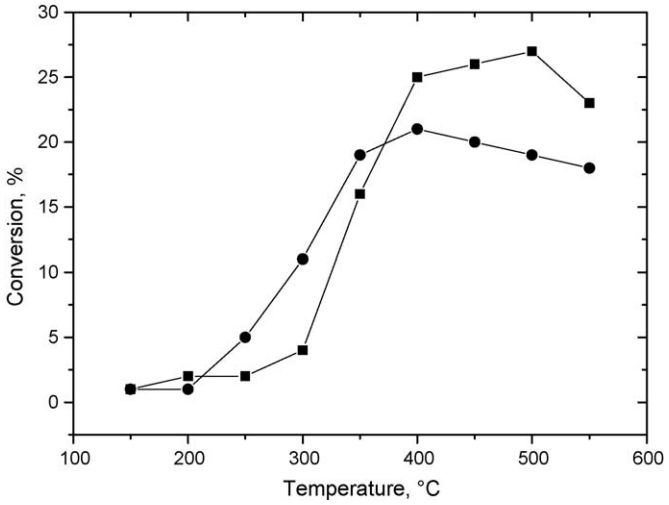

Fig. 3. NO-to-N_2 conversion on the HC-SCR over 1.5 wt.% Ag/alumina-coated microchannels with hexadecane (-●-) and octane (-■-). 500 ppm NO, C1/NO = 6, 6 vol.% O_2, 12 vol.% H_2O and He balance. Total flow 50 ml/min.

3.2. Catalytic testing

Hexadecane was used as a reducing agent. Due to its high cetane number, hexadecane is usually regarded as a high-quality diesel. Moreover, it has been proved by Snåre et al. [22] that hexadecane can be obtained from vegetable oils and fats. The NO to N_2 conversion of the hexadecane-assisted SCR over 1.5 wt.% Ag/alumina-coated microchannels, compared to the reduction obtained with octane is shown in Fig. 3. The reduction activity as hexadecane was used as reducing agent at lower temperatures (<350 °C) resulted higher than when octane was used as reductant (Fig. 3). Theoretical studies of n-alkanes on metal surfaces suggest that the adsorption energies increase linearly with the chain length [23]. The greater enthalpy of adsorption of the longer alkane chains and the weaker C–H bond strength of their methylene groups could at least partially explain their greater ability to react at lower temperatures, when compared to lower alkanes tested in similar systems [3,4,12]. On the other hand, the geometry of the molecule could also have an effect on its reactivity. Hexadecane, with its larger size compared to other components present in diesel fuels, would occupy more space when adsorbed on a metal cluster. Thus, due to steric hindrance, less space would be available for other molecules to adsorb, e.g., NO. The results obtained in the microchannel are similar to those obtained for fixed-bed reactors under similar conditions [20]. However, the benefits of the microchannels compared to larger vessels (reduced homogeneous gas-phase reactions, better heat transfer, higher gas hourly space velocities -GHSV- and intrinsic safety) make the utilization of these devices an excellent tool for kinetic calculations. The details and results of all the performed experiment are found in [21].

3.3. Mathematical modelling

3.3.1. Non-reactive flow

In order to design and use microdevices accurately for research and later for industrial purposes, the behaviour of the gas flow of the reactants and products inside the microchannels has to be characterized and explained. When comparing the flows inside the

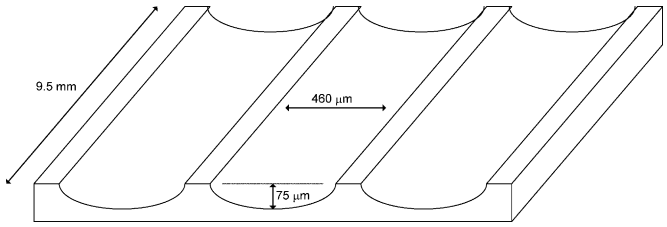

Fig. 4. Schematic view of the catalytic plates (showing three channels out of nine).

microchannels with those present in regular-sized reactors, the differences are as follows: (i) the flow in microchannels is usually laminar and turbulent in macrochannels; (ii) the diffusion paths in the microchannels for heat and mass transfer are very small; (iii) a high surface-to-volume ratio prevails in the microchannels, which implies that a high surface ratio effects dominate over volume effects; and (iv) solid wall materials are important in microchannels, hence, the surface heat transfer is important [1]. Fig. 4 shows a scheme of a microplate (only showing 3 channels out of 9) with their dimensions.

The Knudsen number (Kn) represents the ratio between the main free path of the gas molecules and the characteristic length of the flow domain (diameter of the channel in this case). Calculating the Knudsen number for a system is a usual way for determining the flow regime: when $Kn > 1$, the molecules are most likely to collide with the wall than with other molecules (very small diameters). In this work, under the actual experimental conditions, Knudsen numbers are lower than 10^{-3}. Therefore, continuum flow with no-slip boundary conditions ($Kn < 10^{-2}$, or 10^{-3}) can be assumed and the typical Navier–Stokes (N–S) equations that are valid for macroflows can be applied (Eqs. (1) and (2)).

$$\rho\left(\frac{\partial u_i}{dt} + u_j\frac{\partial u_i}{dx_j}\right) = -\frac{\partial p}{dx_i} + \rho g_i + \frac{\partial}{dx_k} \times \left[\mu\left(\frac{\partial u_i}{\partial x_k} + \frac{\partial u_k}{\partial x_i} - \frac{2}{3}\delta_{ik}\frac{\partial u_j}{\partial x_j}\right)\right] \quad (1)$$

$$\frac{\partial \rho}{dt} + \frac{\partial}{dx_i}(\rho u_i) = 0 \quad (2)$$

The symbols are explained in the Notation section. Eq. (1) represents the velocity profiles of the fluid, whereas Eq. (2) stands for the mass conservation balance. The system of four unknowns and four equations is solved. The equations are a set of coupled differential equations and could, in theory, be solved for a given flow problem by using the methods from traditional calculus. But, in practice, these equations are too difficult to solve analytically. An alternative to solve them is the finite element method (FEM) rendering the partial differential equations (PDEs) into an equivalent ordinary differential equations (ODEs), which are then solved by using standard techniques such as finite differences. For solving the system, implicit time steps and Newton–Raphson iteration was used for convergence, with a tolerance of 10^{-3}.

The system was solved for velocity and pressure and the ideal gas law was used to describe the relationship between pressure and density. The radial coordinate was chosen in the direction of the longer radius (230 μm). Fig. 5 presents the pressure distribution (Fig. 5, left) and velocity distribution normalized with the speed of sound C (Fig. 5, right) along the microchannel at different inlet velocities (P/P_{out} ratio). The velocity and pressure profiles became more prominent when introducing higher flows in the channels. Although these results cannot be validated experimentally due to technical limitations in the microdevice, they are consistent with previously published calculations in similar systems [24].

Recently, high speed computers have been used to solve approximations to the N–S equations using a variety of techniques such as finite difference, finite volume, finite element, and spectral methods (computational fluid dynamics, CFD). The commercial software Comsol Multiphysics 3.5 using a fixed grid was utilized to simulate the flow profile inside the microchannels. Fig. 6 shows the results of the simulations for two different total gas flows: 50 ml/min (Fig. 6, left) and 100 ml/min (Fig. 6, right). The 2D-Navier–Stokes equations were solved with no-slip boundary settings (as the calculated Knudsen number suggested). The density and viscosity of helium were used, i.e., the carrier gas used on the experiments. The calculated mesh consisted in a 2300 elements cell. The flow was solved for the axial (length = 9.5 mm) and width (Ø = 460 μm) dimensions assuming infinite depth on the microchannels. Since the depth of the channels is much shorter than its diameter, the shear stress in the depth dimension should not be very large. The simulations represent the velocity profile of inert gases inside the microchannels. Due to the non-slip conditions, the velocity profile close to the wall becomes zero by definition, obtaining a maximum value in the middle of the microplate (centreline in this case). This non-reactive flow simulation was merely descriptive and the assumptions made were considered acceptable for the purpose of the current contribution. Based on the results presented below in Section 3.3.2.2, the assumptions are considered to remain valid.

The changes in surface velocity for the hypothetical case of 100 ml/min flow are presented in Fig. 6, right. There is an important increase of velocity that would represent a pressure drop inside the reactor. Nonetheless, for the case of total flow 50 ml/min (Fig. 6, left), changes from the inlet surface velocity (0.176 m/s) to the outlet (0.25 m/s) were not very significant and are considered to be low. This consideration is also supported by

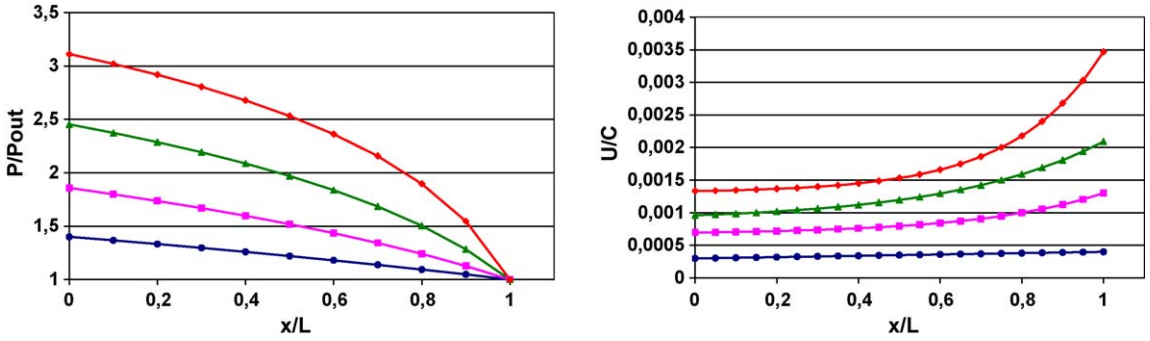

Fig. 5. Normalized modelled pressure (left) and velocity (right) profiles in a microchannel (Ø = 460 μm) for different ratios of P/P_{out} = 1.4 (-●-); 1.9 (-■-); 2.5 (-▲-); and 3.1 (-◆-).

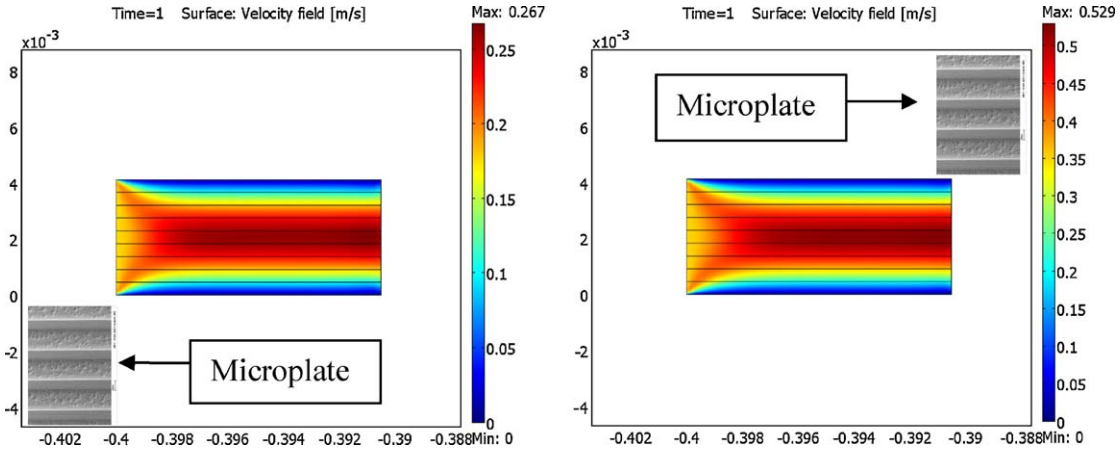

Fig. 6. CFD simulations of an inert flow on a single microplate. 50 ml/min (left), 100 ml/min (right).

Fig. 5, right. A surface velocity of 0.176 m/s is represented by the lowest line (-●-), were the pressure drop is considered to be negligible.

3.3.2. Reactive flow

3.3.2.1. Kinetic modelling with PFR. The detailed kinetic model with PFR is presented with high degree of detail in reference [21]. In the present article, however, the estimated parameters from [21] using PFR model were employed as initial estimates for the laminar flow model with radial diffusion presented in Section 3.3.2.2. Since the results are already published [21] they are omitted from the current work, however, a summary of the findings in [21] is presented. The elementary steps and their rate equations as proposed in [21] are shown in Table 1.

For the mechanism, molecular adsorption of NO and CO are assumed, as well as dissociative adsorption of O_2. The reaction is proposed to occur via intermediates formed by the oxidation of the hydrocarbon, which would further react with adsorbed nitrite or nitrate moieties to produce HC–NO-type species. Molecular nitrogen is suggested to be formed either by combination of two of the HC–NO species or by a reaction between a HC–NO intermediate and pre-adsorbed NO. More details can be found in Ref. [21]. Plug flow reactor model was assumed and the software

Table 1
Proposed reaction mechanism for the $C_{16}H_{34}$-SCR of NOx.

Step	Reaction	Rate equation
1	$NO+^* \Leftrightarrow NO^*$	$r_{+1} = k_{+1} c_{NO} \theta_v$, $r_{-1} = k_{-1} \theta_{NO}$
2	$NO^* + ^* \rightarrow N^* + O^*$	$r_2 = k_2 \theta_{NO} \theta_v$
3	$O_2 + 2^* \Leftrightarrow 2O^*$	$r_{+3} = k_{+3} c_{O_2} \theta_v^2$, $r_{-3} = k_{-3} \theta_O^2$
4	$2N^* \rightarrow N_2 + 2^*$	$r_4 = k_4 \theta_N^2$
5	$NO^* + O^* \rightarrow NO_2 + 2^*$	$r_5 = k_5 \theta_{NO} \theta_O$
6	$CO + ^* \Leftrightarrow CO^*$	$r_{+6} = k_{+6} c_{CO} \theta_v$, $r_{-6} = k_{-6} \theta_{CO}$
7	$CO^* + O^* \rightarrow CO_2 + 2^*$	$r_7 = k_7 \theta_{CO} \theta_O$
8	$C_{16}H_{34} + O^* + ^* \rightarrow C_{16}H_{33}{}^* + OH^*$	$r_8 = k_8 c_{hex} \theta_O \theta_v$
9	$C_{16}H_{33}{}^* + NO^* \rightarrow C_{16}H_{33}NO^* + ^*$	$r_9 = k_9 \theta_{hex} \theta_{NO}$
10	$2C_{16}H_{33}NO^* \rightarrow N_2 + 2C_{16}H_{33}O^*$	$r_{10} = k_{10} \theta_{hex-NO}^2$
11	$C_{16}H_{33}O^* + 48O^* \xrightarrow{fast} 16CO^* + 33OH^*$	
12	$C_{16}H_{33}{}^* + O^* \rightarrow C_{16}H_{33}O^* + ^*$	$r_{12} = k_{12} \theta_{hex} \theta_O$
13	$2OH^* \rightarrow H_2O + O^*$	$r_{13} = k_{13} \theta_{OH}^2$
14	$C_{16}H_{33}NO* + NO* \rightarrow N_2 + C_{16}H_{33}O* + O*$	$r_{14} = k_{14} \theta_{hex-NO} \theta_{NO}$
15	$NO_2 + ^* \Leftrightarrow NO_2{}^*$	$r_{+15} = k_{+15} c_{NO_2} \theta_v$ $r_{-15} = k_{-15} \theta_{NO_2}$
16	$C_{16}H_{33}* + NO_2* \rightarrow C_{16}H_{33}NO* + O*$	$r_{16} = k_{16} \theta_{hex} \theta_{NO_2}$
17	$N^* + CO^* \rightarrow NCO^*$	$r_{17} = k_{17} \theta_N \theta_{CO}$
18	$NCO^* + H_2O \xrightarrow{fast} NH_2{}^* + CO_2$	
19	$NH_2{}^* + NO^* \rightarrow N_2 + H_2O$	$r_{19} = \theta_{NH_2} \theta_{NO}$
20	$N^* + NO^* \rightarrow N_2O^* + ^*$	$r_{20} = k_{20} \theta_N \theta_{NO}$
21	$N_2O^* \xrightarrow{fast} N_2 + O^*$	

ModEst 6.0 [25] was used for obtaining the kinetic parameters. The calculated parameters were used as starting point for the following section in this work (Section 3.3.2.2).

3.3.2.2. Laminar flow model with axial diffusion. Nevertheless of the thickness of the catalytic layer and depending on the reaction conditions, diffusion limitation inside the microchannels might play a role in the system. Moreover, mass transfer limitation from the bulk phase to the surface of the washcoat could appear, mainly via molecular diffusion [14]. When studying reacting flows through microchannels, the traditional approach has been to assume wall-catalyzed reactions. However, as the porous medium acts as a catalyst (being the advantage its higher surface area, thus higher concentration of active sites) the mathematical problem becomes a fully coupled system of equations of reaction, convection and diffusion, which are challenging to solve numerically [26]. Gobby et al. [27] have addressed this problem, developing a model that allows a rapid calculation of some microreacting flows. The purpose of this section was to implement different levels of dynamic modelling, i.e., coupling component mass balances on the catalytic layer with the one in the microchannel. The first step comprised pseudo-homogeneous plug flow model. In case that diffusion limitations appear in the catalytic layer, the model becomes heterogeneous as follows (Eq. (3)):

$$\varepsilon_p \frac{dc_i'}{dt} = r_i \rho_p + \frac{D_e}{\delta^2}\left(\frac{d^2 c_i'}{dx^2} + \frac{s}{x}\frac{dc_i'}{dx}\right), \quad s \in [0,2] \text{ and } x \in [0,1] \tag{3}$$

where the thickness of the catalytic layer (δ) varies along the microchannel (Fig. 2). Other symbols are defined in Notation. The mass balance in the microchannel with diffusion is given by

$$\frac{dc_i(r,l)}{dt} = D_{M,i}\left(\frac{d^2 c_i(r,l)}{dr^2} + \frac{1}{r}\frac{dc_i(r,l)}{dr}\right) - \frac{d(c_i(r,l)w(r))}{dl}, \quad \textit{where,}$$
$$w(r) = 2 \cdot \bar{w}\left(1 - \left(\frac{r}{R}\right)^2\right) \tag{4}$$

which has the boundary conditions $dc_i/dr = 0$ when $r = 0$; $D_e/\delta(dc_i'/dx)_{x=0} = D_{M,i}(dc_i/dr)_{r=R}$; and $(dc_i'/dx)_{x=1} = 0$. For the sake of simplicity, the microchannels were approximated to be circular in Eq. (4) using as a radius the largest distance from the molecules to the catalysts (230 μm, largest channel radius) where the mass transfer limitations could be the highest. This characteristic length for the external mass transfer was kept constant, being 230 μm even larger than half of the hydraulic diameters, thus making the

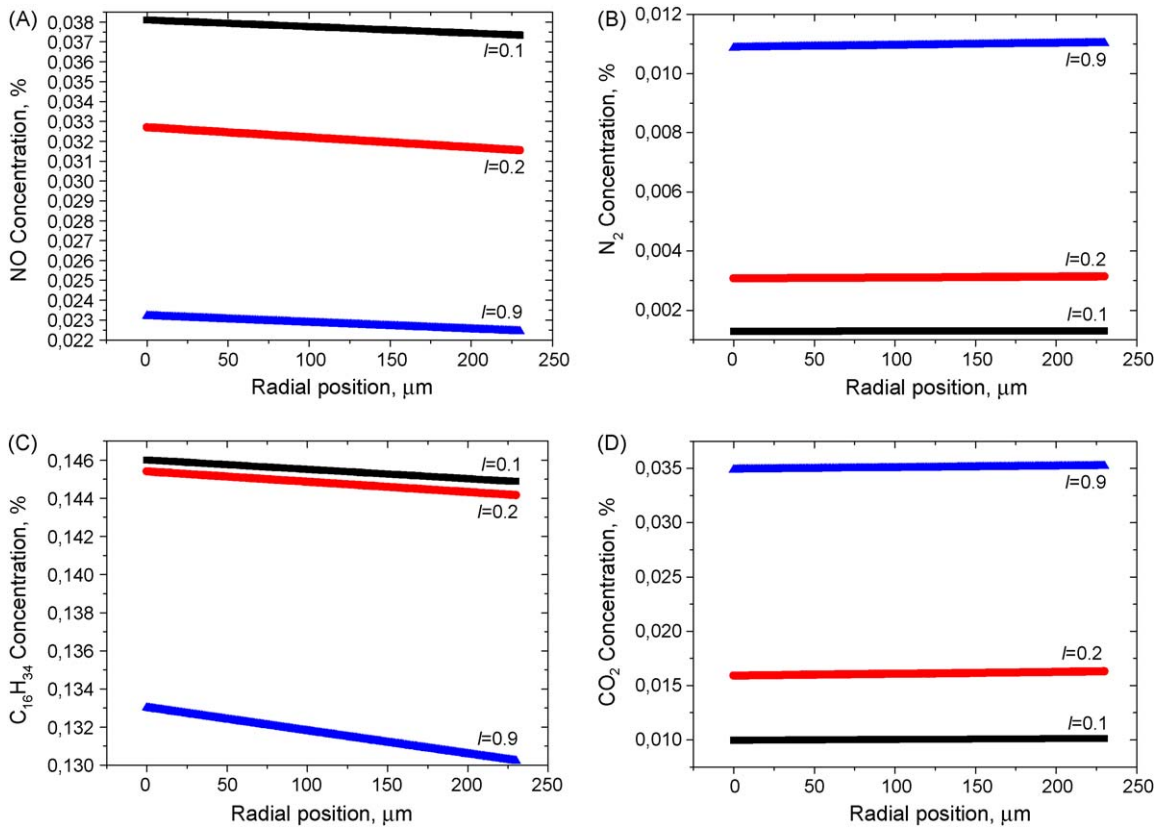

Fig. 7. Radial concentration profiles of the microchannel at different axial positions for NO (A), N_2 (B), $C_{16}H_{34}$ (C) and CO_2 (D).

distance between the molecules with the highest velocity (at the microchannel centre) and the catalytic layer, even larger than in reality, overestimating rather than underestimating the mass transfer effects. For the reactor model, in the axial direction the flow transport was assumed to be by convection and molecular diffusion with Danckwerts boundary condition [28] at the channel entrance and no gradients at the outlet $dc_i(r,l)/dl = 0$ for $l = 1$. Regarding the size of the washcoats, a distribution function $E(\delta)$ depending on the above-mentioned thickness δ can be obtained as well; hence $D_e/\delta(dc_i'/dx)_{x=0}$ can be substituted by $D_e \int_{\delta_{min}}^{\delta_{max}} E(\delta)(dc_i'/dx_\delta)_{x_\delta=0}\, d\delta$, thus Eq. (4) has to be solved for various wall thicknesses (δ).

The dynamic model consisting of a system of partial differential equations was discretized using a finite difference formulation with respect to the spatial coordinate. The resulted ordinary differential equations were solved with an appropriate method for stiff differential equations, e.g., backward difference method to guarantee stability and convergence.

Fig. 7 shows the radial concentration profile for four species at different reactor lengths (0.1; 0.2; and 0.8; normalized lengths). Because of the laminar character of the flow, the molecules at the centre of the channel (with the longest distance to the wall), will have, by definition, the shortest residence time in the reactor, reducing the probability of getting in contact with the catalytic layer. If these molecules would effectively diffuse to the catalytic layer (as the radial concentration profiles suggested, Fig. 7), the external mass transfer limitations are considered insignificant. The calculated concentration gradient in the bulk phase was negligible, even considering the largest channel radius possible (230 μm). The results from the reactor model (Fig. 7), showed no depletion or augment of the species at the channel wall compared to the bulk phase, thus the mass transfer from the bulk phase to the catalyst layer is fast and effective. Fig. 7 also shows that close to the inlet, the radial profile is somehow flatter than the one close the outlet, when fully developed flow is expected. Moreover, because of the laminarity of the flow in microdevices, the external mass transfer should only be dependent on molecular diffusion. It is believed that most of the diffusion would occur from the gas phase to the solid film. Since the diffusion path from the centre of the microchannel to the catalytic layer (230 μm at its maximum) is much larger than the internal mass transfer (in the washcoat, 20 μm at its maximum), it is reasonable to assume that no mass transfer limitations inside the catalytic layer are present. Consequently, the estimated parameters found in [21] by using a simple PFR model are considered as valid, corresponding to kinetically controlled regime. In general, the results described very well the behaviour of gas-phase SCR of NOx over Ag/alumina.

4. Conclusions

Microchannels washcoated with alumina were successfully impregnated with an active 1.5 wt.% silver. The silver distribution along the microchannels was found to be uniform. Continuous NO reduction by hydrocarbons in excess oxygen was investigated over the impregnated microchannels in the temperature range 150–550 °C. Hexadecane was used as reducing agent for the HC-SCR of NOx showing reasonable levels of reduction.

Non-reactive flow description inside the channels was performed by using the Navier–Stokes equations and pressure and velocity profiles inside the microchannels were theoretically obtained. The non-reactive flow was also evaluated by CFD simulations, showing only small pressure drops for the studied flows.

Finally, the reactive flow was investigated by using a mathematical laminar flow model with radial diffusion and diffusion in the catalyst layer for the hexadecane-SCR of NOx. The radial concentration profiles for the reactants (NO and $C_{16}H_{34}$)

and the products (N_2 and CO_2) are presented. The findings suggest that the radial diffusion on the channels was reasonably small. Hence, the diffusion effect on the catalytic layer was estimated to be rather minor and the use of a simple PFR model for the microchannels becomes valid.

Notation

C	speed of sound
c_i	concentration of species in the bulk phase
c'_i	concentration of species in the catalyst layer
D_e	effective diffusion coefficient
$D_{M,I}$	molecular diffusion coefficient
g_i	component i of the gravity
Kn	Knudsen number
l	axial coordinate
p	total pressure
R	reactor radius
r	radial coordinate
r_i	reaction rates
s	form factor
t	time
u_i	component i of the flow velocity
$w(r)$	flow velocity in the l direction
$\bar{w}$	average flow velocity
x	radial coordinate along the washcoat depth
x_i	physical coordinate in the i-direction
δ	thickness of the catalytic layer
$\delta_{i,k}$	Kronecker delta $\begin{cases} i = k \rightarrow 1 \\ i \neq k \rightarrow 0 \end{cases}$
ε_p	porosity of the coating
μ	dynamic viscosity
ρ	fluid density
ρ_p	density of the catalyst particle

Acknowledgements

The financial support from the Graduate School on Chemical Engineering for J.R. Hernández Carucci is gratefully acknowledged. This work is part of the activities at the Åbo Akademi Process Chemistry Centre within the Finnish Centre of Excellence Programme (2006–2011) appointed by the Academy of Finland.

References

[1] W. Ehrfeld, V. Hessel, H. Löwe, Microreactors—New Technology for Modern Chemistry, Wiley-VCH, Weinheim, 2000.
[2] L. Rantanen, R. Linnaila, P. Aakko, T. Harju, SAE Paper No. 2005-01-3771, 2005.
[3] K. Eränen, L.-E. Lindfors, F. Klingstedt, D.Yu. Murzin, J. Catal. 219 (2003) 25.
[4] F. Klingstedt, K. Eränen, L.-E. Lindfors, S. Andersson, L. Cider, C. Landberg, E. Jobson, L. Eriksson, T. Ilkenhans, D. Webster, Top. Catal. 30/31 (2004) 27.
[5] K. Eränen, L.-E. Lindfors, A. Niemi, P. Elfving, L. Cider, SAE Paper 2000-01-2813, 2000.
[6] L. Čapek, K. Novoveská, Z. Sobalík, B. Wichterlová, L. Cider, E. Jobson, Appl. Catal. B 60 (2005) 201.
[7] L. Čapek, J. Dědeček, B. Wichterlová, L. Cider, E. Jobson, V. Tokarová, Appl. Catal. B 60 (2005) 147.
[8] P. Konova, K. Arve, F. Klingstedt, P. Nikolov, A. Naydenov, N. Kumar, D.Yu. Murzin, Appl. Catal. B 70 (2007) 138.
[9] S. Satokawa, Chem. Lett. (2000) 294.
[10] J. Shibata, K-i. Shimizu, S. Satokawa, A. Satsuma, T. Hattori, Phys. Chem. Chem. Phys. 5 (2003) 2154.
[11] R. Burch, J.P. Breen, C.J. Hill, B. Krutzsch, B. Konrad, E. Jobson, L. Cider, K. Eränen, F. Klingstedt, L.-E. Lindfors, Top. Catal. 30/31 (2004) 19.
[12] R. Burch, J.P. Breen, F.C. Meunier, Appl. Catal. B 39 (2002) 283.
[13] R.E. Hayes, S.T. Kolaczkowski, Chem. Eng. Sci. 49 (1994) 3587.
[14] R.E. Hayes, B. Liu, R. Moxom, M. Votsmeier, Chem. Eng. Sci. 59 (2004) 3169.
[15] E. Tronconi, P. Forzatti, J.P. Gomez Martin, S. Mallogi, Chem. Eng. Sci. 47 (1992) 2401.
[16] R. Giudici, E. Tronconi, Int. J. Heat Mass Transf. 39 (1996) 1963.
[17] G. Groppi, E. Tronconi, Chem. Eng. Sci. 52 (1997) 3521.
[18] S.R. Dhanushkodi, N. Mahinpey, M. Wilson, Process Saf. Environ. Prot. 86 (2008) 303.
[19] R. Zapf, C. Becker-Willinger, K. Berresheim, H. Bolz, H. Gnaser, V. Hessel, G. Kolb, P. Loeb, A.-K. Pannwitt, A. Ziogas, Trans. IChemE 81 (2003) 721.
[20] J.R. Hernández Carucci, K. Arve, K. Eränen, D. Yu Murzin, T. Salmi, Catal. Today 133–135 (2008) 448.
[21] J.R. Hernández Carucci, A. Kurman, H. Karhu, K. Arve, K. Eränen, J. Wärnå, T. Salmi, D.Yu. Murzin, Chem. Eng. J. (2009), doi:10.1016/j.cej.2009.01.031.
[22] M. Snåre, I. Kubičková, P.-M. Arvela, K. Eränen, D.Yu. Murzin, Catal. Org. React. 115 (2006) 415.
[23] S.M. Wetterer, D.J. Lavrich, T. Cummings, S.L. Bernasek, G. Scoles, J. Phys. Chem. B 102 (1998) 9266.
[24] S. Roy, R. Raju, J. Appl. Phys. 93 (2003) 4870.
[25] H. Haario, ModEst 6. 0—A User's Guide, ProfMath, Helsinki, 2007.
[26] S. Hardt, in: F.J. Keil (Ed.), Modeling and Simulation of Microreactors in Modeling of Process Intensification,, Wiley-VCH, Weinheim, 2007.
[27] D. Gobby, I. Eames, A. Gavriilidis, Proc. IMRET 5: 5th Int. Conf. on Microreaction Tech., Strasbourg, France, May 2001, Springer-Verlag, Berlin, 2001, p. 141.
[28] P.V. Danckwerts, Chem. Eng. Sci. 2 (1953) 1.